Its overall length is 320 mm. The small signal isolations of this circulator are better than 20 dB between all isolated ports over 8.5–9.6 GHz with a small signal insertion loss below 0.20 dB over the temperature range −40–+100°C.

Fig. 9 indicates the large signal insertion loss of the differential phase shift circulator at a peak power level of 1 MW at a frequency of 9.6 GHz. The pulsewidth of the signal was 0.16 μs and its duty cycle was 0.001.

It is seen from the above results that not only is the insertion loss of the device independent of signal level up to 1-MW peak but also that this biasing condition minimizes the magnetic losses of the material due to the suppression of both small and large signal coupling between the microwave signal and the spinwave manifold.

VIII. Conclusions

This paper has described the successful design of a 1-MW differential phase shift circulator using ferrite sections biased at a direct magnetic field between the subsidiary and main resonances. Although the final device has been evaluated at 1 MW (500 kW through each phase shift section), the individual phase shift sections exhibited no nonlinear loss at 1-MW peak. This proves the design of such a circulator to a power rating of 2-MW peak. The overall insertion loss of the final device was 0.18 dB at 9.6 GHz.

Acknowledgment

The authors would like to thank Ferranti Ltd., Dundee, for permission to publish this paper.

References

[1] R. W. Damon, "Relaxation effects in ferromagnetic resonance," *Rev. Mod. Phys.*, vol. 25, pp. 239–45, 1953.
[2] H. Suhl, "The non-linear behaviour of ferrites at high signal level," *Proc. Inst. Radio Engrs.*, vol. 44, p. 1270, 1956.
[3] E. Schlömann, "Ferromagnetic resonance at high power levels," Raytheon Technical Report R-48, 1959.
[4] A. Lagrange, H. Lahmi, and B. R. Vallatin, "*K*-band high-peak-power junction circulator: Influence of the static magnetic field," *IEEE Trans. Magnetics*, vol. Mag-9, pp. 531–534, Sept. 1973.
[5] C. R. Buffler, *J. Appl. Phys.*, vol. 30, p. 1725, 1959.
[6] Q. H. F. Vrehen, G. H. Beljers, and J. G. M. de Lau, "Microwave Properties Fine-Grain Ni and Mg Ferrites," *IEEE Trans. Magnetics*, MAG-5, pp. 617–621, 1969.
[7] C. Kittel, "On the theory of ferromagnetic resonance absorption," *Phys. Rev.*, vol. 73, pp. 155–161, 1948.

Design Considerations of Broadband Dual-Mode Optical Fibers

JUN-ICHI SAKAI, KENICHI KITAYAMA, MEMBER, IEEE, MASAHIRO IKEDA, MEMBER, IEEE, YASUYUKI KATO, AND TATSUYA KIMURA, MEMBER, IEEE

Abstract—**We propose and present design data for a new type of graded index fiber which has a profile and radius such that only two mode groups (LP_{01} and LP_{11}) propagate and both propagate with virtually identical group velocities. This dual-mode fiber has a core diameter approximately twice that of a conventional step-index single-mode fiber. For example, a core diameter of 16.3 μm is attainable with relative index difference $\Delta = 0.3$ percent at 1.25-μm wavelength. Fabrication tolerances securing a group delay difference below 100 ps/km are given by a power-law profile parameter $\alpha = 4.85 \pm 0.25$ and a normalized frequency $v = 4.45 \pm 0.11$. The allowable v-value deviation range to keep the group delay difference within 100 ps/km is about five times as large as that of a step-index fiber, in which group delays of two mode groups are matched. Comparison with a multimode graded-index fiber, with respect to group delay characteristics and bending loss of the dual-mode fiber, are also discussed.**

Manuscript received November 10, 1977; revised February 6, 1978.

J. I. Sakai and T. Kimura are with the Musashino Electrical Communication Laboratory, Nippon Telegraph and Telephone Public Corporation, Musashino-shi, Tokyo, 180, Japan.

K. Kitayama, M. Ikeda, and Y. Kato are with the Ibaraki Electrical Communication Laboratory, Nippon Telegraph and Telephone Public Corporation, Tokai, Ibaraki, 319-11, Japan.

I. Introduction

SINGLE-MODE optical fibers are expected to offer a promising means for large-capacity optical transmission. However, technical difficulties in fiber splicing and coupling seem to have blocked their utilization, because the core diameter is as small as several microns. Several methods to enlarge the core diameter have been devised.

One method is to decrease the relative index difference Δ between core and cladding. It has been reported that Δ has been lowered to the order of 0.1 percent [1]. However, the bending losses increase with decreasing Δ. Another recognized method is to use an optical carrier with longer wavelengths [2] than the currently used 0.8–0.9 μm. When the carrier wavelength is chosen between 1.0 and 1.6 μm,

0018-9480/78/0900-0658$00.75 ©1978 IEEE

the core diameter can be increased by about 20–90 percent, as compared with values at the 0.85-μm wavelength.

Another method for enlarging the core diameter is to change the refractive index profile. $W-$ [3], combined $M-W$ [4], and ring-shaped [5] index fibers have been proposed. The first type of profile permits enlarged core diameter without noticeable bending loss increase. On the contrary, the last two types of fibers suffer relatively large bending loss because their fields decay gradually in the cladding layer.

We propose a dual-mode fiber (see also [6], [7]) to realize a large-core broadband fiber. It carries only two guided mode groups below cutoff with a greatly reduced group delay difference. The core diameter is made about twice as large as that of a conventional single-mode fiber. Consequently, splicing and coupling difficulties can be reduced while favorable broadband characteristics are retained.

After a detailed description of the dual-mode fiber design principle in Sections II and III discusses tolerance limits which may be inevitable in practical fiber fabrication. Modal dispersion resulting from possible deviations in the profile parameters is compared with that of a multimode graded-index fiber in Section IV. Finally, bending loss is compared with a conventional step-index single-mode fiber.

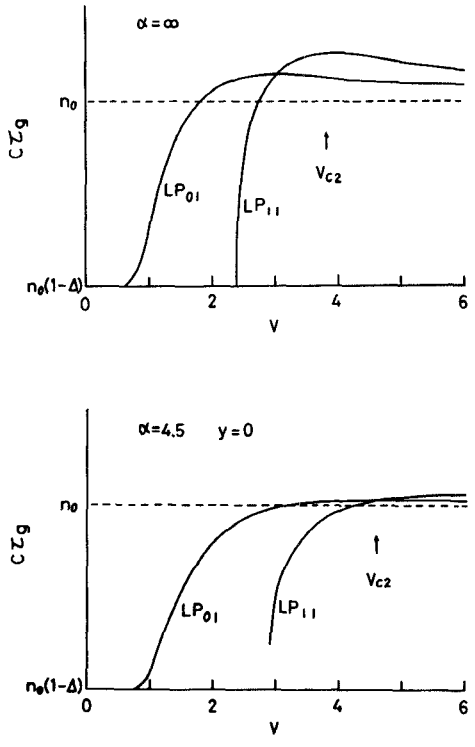

Fig. 1. Group delay τ_g for the LP_{01} and LP_{11} modes. (a) Step-index fiber. (b) Dual-mode fiber with $\alpha=4.5$ and $y=0$. v_{c2} indicates the cutoff of the LP_{21} mode.

II. Design Principle

The fiber structure to be discussed in this paper is based on the following design principles.

1) The first higher order modes (TE_{01}, TM_{01}, and HE_{21}, or LP_{11} in the linearly polarized mode representation [8]) are allowed to propagate simultaneously with the dominant mode (HE_{11} or LP_{01}).

2) Group delays of the LP_{01} and LP_{11} modes coincide at $v=v_0$. Here, a normalized frequency v is defined as $2\pi a n_0(2\Delta)^{1/2}/\lambda$ in a weakly guiding approximation [8], where a is the core radius, n_0 is the index of the core center, Δ is the relative index difference between core and cladding, and λ is the wavelength.

3) The normalized frequency v_0 is raised to just below cutoff v_{c2} of the second higher order modes (EH_{11} and HE_{31}, or LP_{21}) by proper choice of the core index profile.

Even in a step-index fiber, the group delay of the LP_{01} mode agrees with that of the LP_{11} mode in the vicinity of $v=3.0$, as shown in Fig. 1(a). However, this v value is considerably smaller than $v_{c2}=3.83$ for the step-index profile, and the condition for eliminating the group delay difference between both modes is critical. Conditions for group delay matching with increased fabrication tolerance are derived below, assuming that the index profile varies by an α-power law.

Assuming that Δ is small enough to permit the weakly guiding approximation, the core and cladding index distribution is represented as

$$n(r)=\begin{cases} n_0[1-\rho\Delta(r/a)^\alpha] & (0\leqslant r\leqslant a) \\ n_0(1-\Delta) & (r>a) \end{cases} \quad (1)$$

where both α and ρ are constants characterizing index distribution. A variational method has been applied to analyze the propagation problems in inhomogeneous index profile fibers [9]. The group delay τ_g, of the LP_{01} and LP_{11} modes, is numerically calculated by using a method proposed in [9], as shown in Appendix I. For the moment, $\rho=1$ is assumed.

Fig. 1(b) illustrates the numerical solution for group delay in the LP_{01} and LP_{11} modes, when $\alpha=4.5$ and $y=0$. Here, the index difference dispersion parameter [10] y is defined by $-(2n/N)(\lambda/\Delta)(d\Delta/d\lambda)$, where N is the group index. Group delays of these modes are matched at $v_0=4.605$, which corresponds to v_{c2}. Thus the modes of Fig. 1(b) satisfy the preceding design principle. The values of α and v, where the preceding design principle is satisfied, are called optimum values. By comparing Figs. 1(a) and (b), it is found that the change in group delay difference with $\alpha=4.5$ is smaller than that of a step-index fiber ($\alpha=\infty$), for v deviation. By further reducing the value of α, the value of v_0 exceeds the LP_{21} mode cutoff v_{c2}.

The ratio v_0/v_{c2} versus α is depicted in Fig. 2 for $y=0$. The ratio v_0/v_{c2} increases rapidly near $\alpha=2.0$ and approaches 0.79 asymptotically at large α. Since the value of v_0 becomes equal to that of v_{c2} at $\alpha=4.5$, the value of α should be chosen larger than 4.5, to keep LP_{21} mode cutoff.

The relation between α and v, required to give a constant group delay difference $\delta\tau_g$ between the LP_{01} and LP_{11} modes, is shown in Fig. 3 for $y=0$ and $\Delta=0.3$ percent. The two curves representing $\delta\tau_g=0$ and v_{c2}, cross at $\alpha=4.5$ and $v=4.605$. When the required group delay difference is less than 100 ps/km and the core diameter is

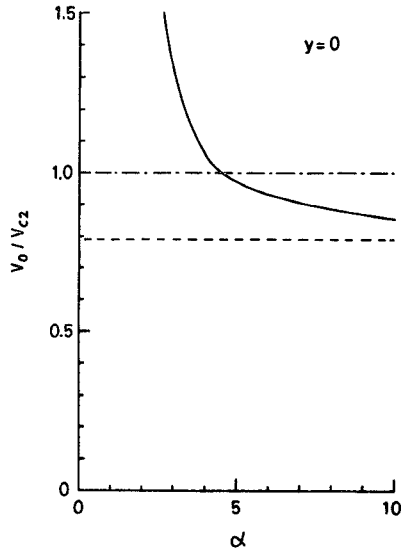

Fig. 2. Ratio of v_0 to v_{c2} versus α. $y=0$. v_0 denotes the v value where the group delay of the LP_{01} mode equals that of the LP_{11} mode. v_{c2} is the cutoff v value of the LP_{21} mode.

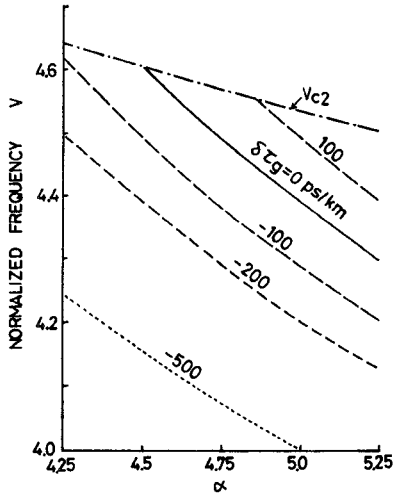

Fig. 3. Tolerable ranges for α and v giving constant group delay difference $\delta\tau_g$ between the LP_{01} and LP_{11} modes. $\rho=1$. $n_0=1.45$. $\Delta=0.3$ percent. $y=0$. v_{c2} is the LP_{21} mode cutoff.

desired to be as large as possible, tolerable ranges of α and v are given approximately by 4.85 ± 0.25 and 4.45 ± 0.11, respectively. The tolerable range for v is about five times as large as that of a step-index profile. Fabrication tolerances will be described in detail in the next section.

Core diameters of several broadband fibers at $\lambda=1.25$ μm are given in Fig. 4 as a function of Δ. The core diameter of a fiber with $\alpha=4.5$ and $\Delta=0.3$ percent will be 16.3 μm, which is about twice as large as that of a step-index single-mode fiber with the same Δ. When $\rho=2$, a similar procedure shows that the optimum α is about 3, and the normalized frequency v can be raised to 6. The core diameter for $\rho=2$ is also shown in Fig. 4. The core diameter of the W fiber for $v=3.6$ is similarly shown for comparison.

The above arguments are based on the assumption of power-law profile. Effects of deviations from the power-law, such as profile of other functional form, an index dip at the core center and profile irregularity, remain to be studied.

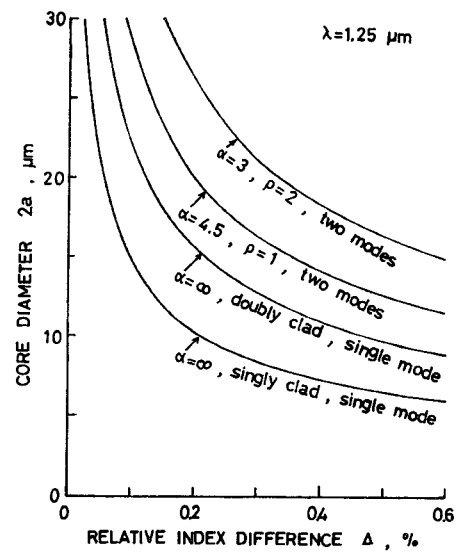

Fig. 4. Core diameters of several broadband fibers as a function of relative index difference Δ. $\lambda=1.25$ μm. $n=1.45$.

III. Optimum Value and Fabrication Tolerance

In the preceding section, group delay characteristics were treated only for $y=0$ to explain the design principle. The group delay τ_g is determined by the fiber parameters given in Appendix I. Among these parameters, x and Q depend on fiber structure, while N, Δ, and y depend on the material of core and cladding. This section reports a practical design which takes account of material effect.

In (A1) x and Q are, at most, of the order of unity, and $|y|$ is usually smaller than unity, as will be shown later. Since Δ is much smaller than unity, expansion of (A1) into a power series, in terms of Δ, leads to the following relation on group delay difference $\delta\tau_g$.

$$\begin{aligned}\delta\tau_g &= \tau_g(LP_{11}) - \tau_g(LP_{01}) \\ &= (N/c)\left[\Delta\left[\{1-(1+y/4)Q_1\}x_1 - \{1-(1+y/4)Q_0\}x_0\right]\right. \\ &\quad + \Delta^2\left[\{3/2-(1+y/4)Q_1\}x_1^2\right. \\ &\quad \left.\left. - \{3/2-(1+y/4)Q_0\}x_0^2\right]\right] + 0(\Delta^3). \qquad (2)\end{aligned}$$

Suffixes 0 and 1 indicate the LP_{01} and LP_{11} modes, respectively.

The group delay difference is proportional to the group index N, which, however, is not involved in the determination of optimum conditions. The value of N is insensitive to dopant species and wavelength. It is expected that the optimum values of α and v will depend more strongly on y than on Δ, while the tolerance range depends on Δ rather than y. Of these three parameters, the wavelength dependence of y gives the largest effects in optimizing α and v. To gain generality y is chosen as a parameter indicating material effects in the following discussion.

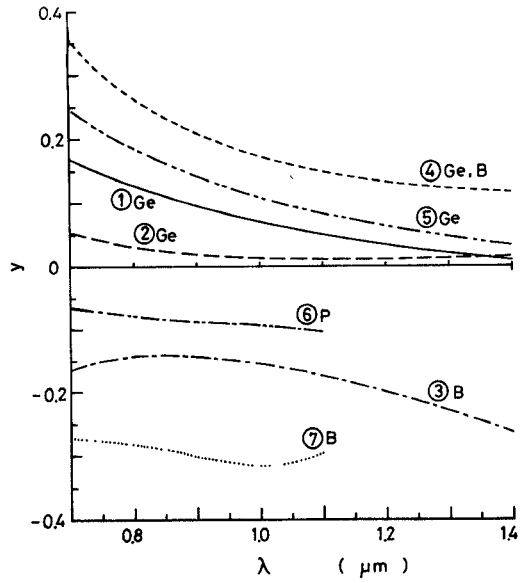

Fig. 5. Wavelength dependence of index difference dispersion parameter y. Each fiber material is listed in Table I.

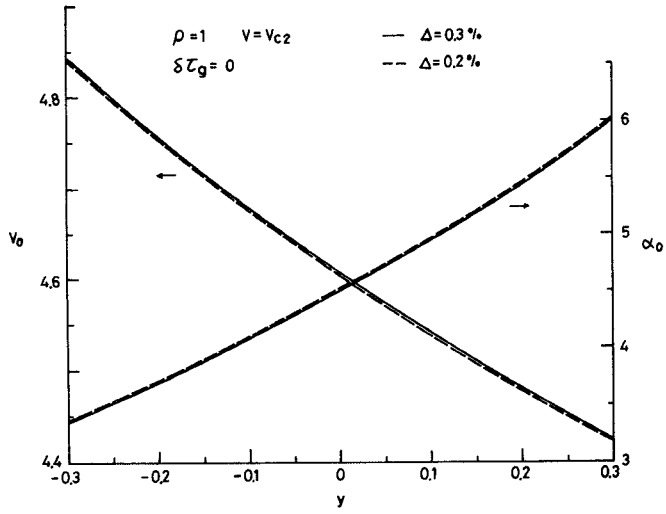

Fig. 6. Dependence of optimum values α_0 and v_0 on y. Group delay difference $\delta\tau_g=0$. $\rho=1$. $v=v_{c2}$. v_{c2} denotes the cutoff of the LP_{21} mode. Solid lines indicate the value with $\Delta=0.3$ percent and broken lines indicate $\Delta=0.2$ percent.

Published results on the wavelength dependence of y are depicted in Fig. 5 for several combinations of silica-based core and cladding material. Fiber material compositions are listed in Table I. The Δ value of each fiber at $\lambda=1.05$ μm is also shown for reference. The value of y ranges mostly between 0.3 and -0.3 in the 0.7–1.4-μm wavelength region.

The dependence of the optimum values, α_0 and v_0, on y is shown in Fig. 6 for $\Delta=0.2$ and 0.3 percent. As stated previously, the optimum values depend more strongly on y rather than on Δ. For example, when Δ shifts from 0.2 to 0.3 percent at $y=0$, the values of α_0 and v_0 deviate only by 0.2 and 0.03 percent, respectively.

The core diameter $2a$ at $\lambda=1.25$ μm is plotted in Fig. 7 as a function of Δ and y for the optimum values, α_0 and v_0 of α and v. The optimum core diameter at different

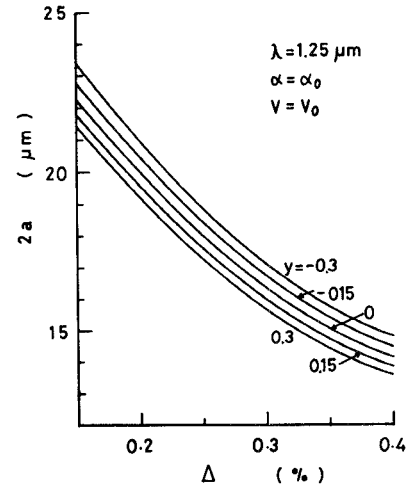

Fig. 7. Core diameters for optimum α and v values with a given y as a function of relative index difference Δ. $\rho=1$. $\lambda=1.25$ μm. $n_0=1.45$.

TABLE I
FIBER MATERIAL WITH SEVERAL SILICATE GLASSES

Sample	Core Dopant (mol.%)			Cladding Dopant (mol.%)		Δ (%) at 1.05 μm	Ref.
	GeO_2	B_2O_3	P_2O_5	GeO_2	B_2O_3		
1	3.1	-	-	-	-	0.32	11
2	3.5	-	-	-	-	0.38	11
3	-	-	-	-	3.5	0.16	12
4	2.2	3.3	-	-	-	0.16	12
5	7.9	-	-	5.8	-	0.23	11
6	-	-	4.0	-	-	0.30	13
7	-	-	-	-	4.2	0.27	13

wavelengths is easily calculated by using the relation that $2a$ is proportional to λ.

It is also important in fiber fabrication to know the material dependence of fabrication tolerances. When a deviation δv of v corresponds to the group delay difference $\delta\tau_g$ and it is desired that the core diameter be as large as possible, v is designed by v^* obtained in the equation

$$v^*(\alpha)+\delta v=v_{c2}(\alpha). \tag{3}$$

The δv corresponding to $\delta\tau_g=-100$ ps/km is shown in Fig. 8 as a function of Δ and y for $\alpha=\alpha_0$ and $N=1.45$. The range $|\delta v|$ decreases with Δ and is nearly proportional to $\delta\tau_g$ when $\delta\tau_g$ is small. This property is useful to obtain δv for other $\delta\tau_g$ values from Fig. 8.

When an α deviation $\delta\alpha$ corresponds to a given $\delta\tau_g$, the designed α-value α^* is obtained similarly:

$$\alpha^*(v_{c2})+\delta\alpha=\alpha_0(v_{c2}). \tag{4}$$

The $\delta\alpha$ corresponding to $\delta\tau_g=100$ ps/km is given in Fig. 9 as a function of Δ and y for $v=v_0$. The $\delta\alpha$ decreases as Δ increases. It is readily expected, from (2), that the tolerable ranges of v and α decreases with Δ.

Let us show the refractive index distribution which takes into account the tolerable ranges, δv and $\delta\alpha$. The curve of constant group delay difference with $y=0$ was

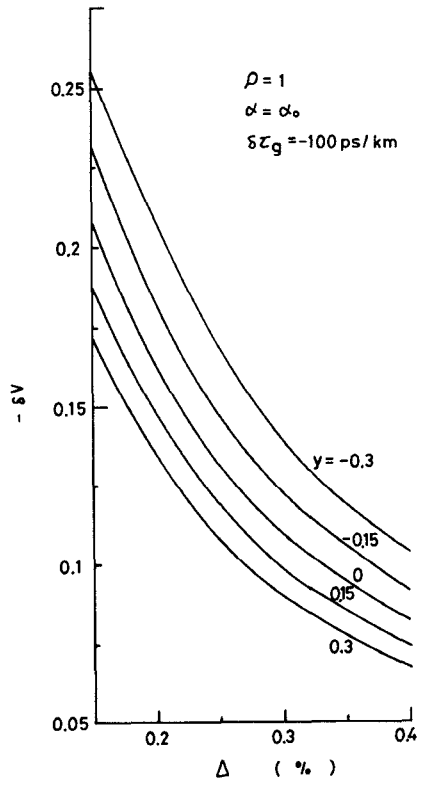

Fig. 8. V value deviation δv corresponding to group delay difference $\delta\tau_g = -100$ ps/km. $\rho = 1$. α value is optimum for each y. $N = 1.45$.

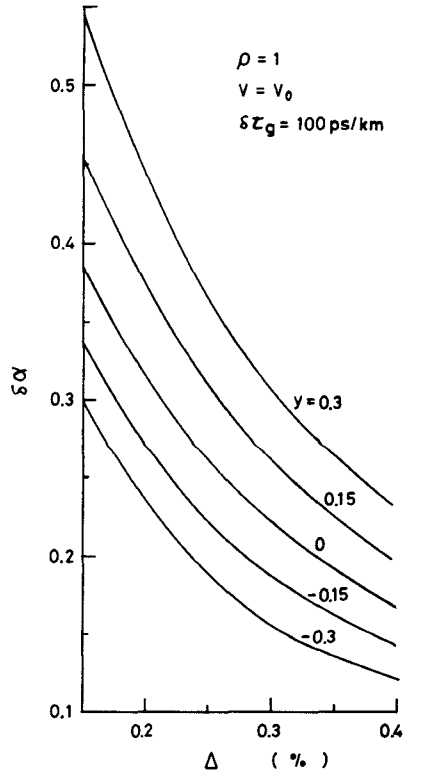

Fig. 9. α-value deviation $\delta\alpha$ corresponding to group delay difference $\delta\tau_g = 100$ ps/km. $\rho = 1$. V value is optimum for each y. $N = 1.45$.

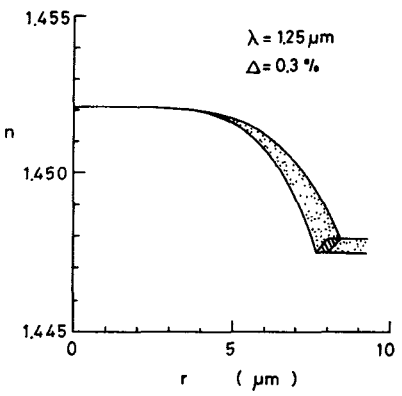

Fig. 10. Example of refractive-index profile taking account of fabrication tolerances. $\delta\tau_g \leqslant 100$ ps/km. $v = 4.45 \pm 0.11$. $\lambda = 1.25$ μm. $n_0 = 1.4521$. $\Delta = (0.3 \pm 0.015)$ percent. The combination of core radius a and relative index difference Δ is permitted in the hatched region. $a = 7.87$ μm.

previously given in Fig. 3. The tolerable ranges of α and v for $\delta\tau_g \leqslant 100$ ps/km, are approximately 4.85 ± 0.25 and 4.45 ± 0.11, respectively. Let the tolerable values for a (μm) and Δ (percent) be δa and $\delta\Delta$, respectively. The relation between δa and $\delta\Delta$ for $\lambda = 1.25$ μm and $n_0 = 1.4521$ is obtained by

$$\left| \frac{\delta a}{0.1946} + \frac{\delta\Delta}{0.0148} \right| \leqslant 1 \qquad (5)$$

as shown in Appendix II. The refractive index profile with $\Delta = (0.3 \pm 0.015)$ percent is depicted in Fig. 10. The combination of a and Δ is permitted only in the hatched region. Incidentally, $a = 7.87$ μm and the maximum value of δa is 0.40 μm.

The effect of material and waveguide dispersion [14], that is wavelength dispersion, can not always be neglected when an intermodal dispersion is relatively small. When the fiber is composed of material 1 in Table I, the dispersion of the LP_{01} and LP_{11} modes differs by about 2 ps/(km·nm) for $\alpha = 4.5$ and $v = v_{c2} = 4.6$. In the 1.2–1.4-μm range, wavelength dispersion is within 10 ps/(km·nm) [6]. As long as the spectral optical carrier width is sufficiently narrow, the wavelength dispersion effect can be ignored.

IV. Comparison with Multimode Graded-Index Fibers

The α value tolerance of the dual-mode fiber is compared with that of a multimode graded- index fiber in this section. When $y = 0$ and one percent deviation in v value is permitted, designed values α^* and v^* become 4.64 and 4.54, respectively, by using Fig. 2. Fig. 11 illustrates the group delay difference for $\alpha = 4.872$ and 4.408, which correspond to ± 5 percent in α deviation from $\alpha = 4.64$, as well as for $\alpha = 4.64$ with $\Delta = 0.3$ percent. The ordinate on the left side denotes group delay difference $\delta\tau_g$, where $\delta\tau_g = 0$ corresponds to the value at $v = v^* = 4.64$. The $\delta\tau_g$ values at $\alpha = 4.872$ and 4.408 are 98 ps/km and -91 ps/km, respectively.

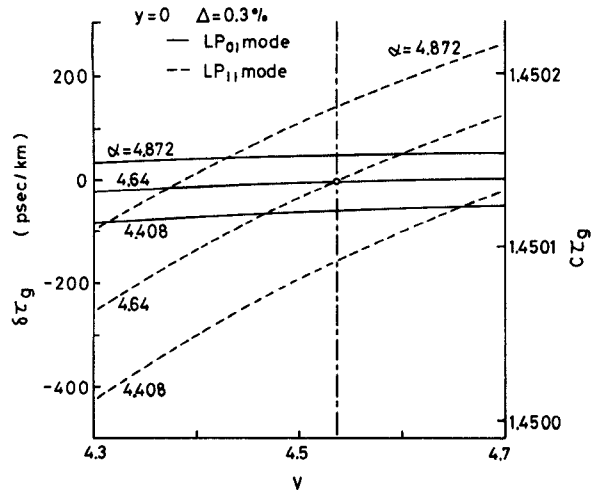

Fig. 11. Group delay difference $\delta\tau_g$ caused by 5-percent deviation in profile parameter from designed value $\alpha^* = 4.64$. $y = 0$. $\Delta = 0.3$ percent. $N = 1.45$.

The rms pulsewidth 2σ due to intermodal broadening in a multimode graded-index fiber is given by [10]

$$2\sigma = \frac{N\Delta}{c} \cdot \frac{\alpha}{\alpha+1}\left(\frac{\alpha+2}{3\alpha+2}\right)^{1/2} \cdot \left[C_1^2 + \frac{4C_1C_2\Delta(\alpha+1)}{2\alpha+1} + \frac{4\Delta^2C_2^2(2\alpha+2)^2}{(5\alpha+2)(3\alpha+2)}\right]^{1/2} \quad (6)$$

where

$$C_1 = (\alpha-2-y)/(\alpha+2)$$
$$C_2 = (3\alpha-2-2y)/[2(\alpha+2)] \quad (7)$$

and y is the index difference dispersion parameter, as mentioned earlier. The value of 2σ given by (6) is minimized at $\alpha = 2+y$. The minimum value of 2σ is about 140 ps/km for $y = 0$ and $\Delta = 1$ percent. When 5-percent α deviation is permitted, 2σ becomes larger than 670 ps/km.

It can be seen that the minimum value of the pulse broadening is zero in the dual-mode fibers, while it is 140 ps/km in highly multimode graded-index fibers. The dual-mode fibers have tolerances more than seven times as large as multimode graded-index fibers, with respect to α deviation.

V. Bending Loss

Bending loss is important in determining the lower limit of relative index difference. A bending loss formula has been derived for fibers with arbitrary inhomogeneous cross section [15]. A numerical calculation method was developed to evaluate the bending loss of fibers with an axially symmetric arbitrary profile by using a staircase index approximation [16].

The radius of curvature R^*, at which the bending loss exceeds 0.1 dB/km, is shown in Fig. 12 for the LP_{01} and LP_{11} modes with $\alpha = 4.5$, $v = v_{c2} = 4.6$, and $\lambda = 1.25$ μm.

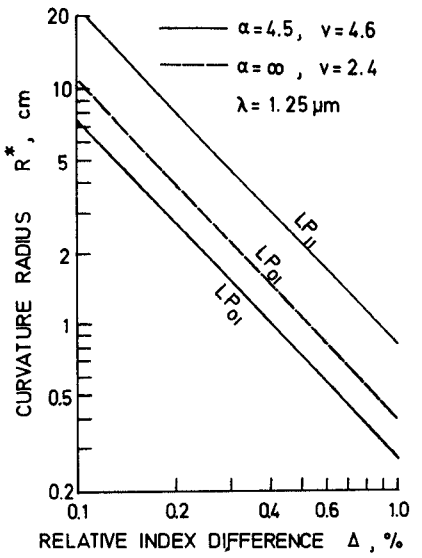

Fig. 12. Permissible bending radius R^* versus relative index difference Δ. $\lambda = 1.25$ μm. $n_0 = 1.45$. Bending loss is assumed to be 0.1 dB/km. Solid lines indicate the values for the LP_{01} and LP_{11} modes of the dual-mode fiber with $\alpha = 4.5$ and $v = 4.6$, while broken line indicates the value for the LP_{01} mode of the step-index fiber with $v = 2.4$.

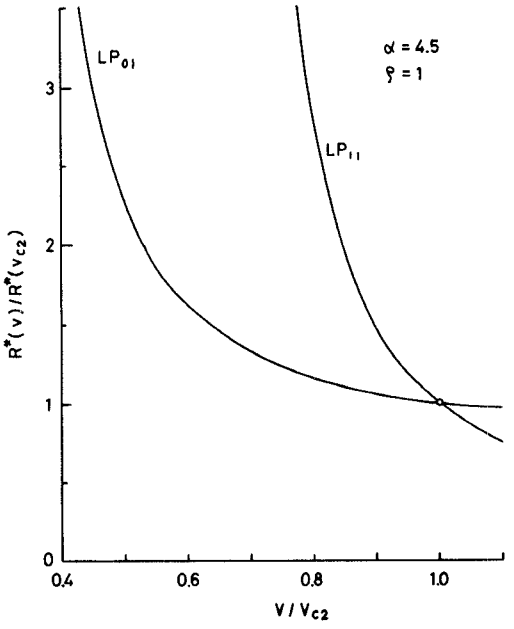

Fig. 13. Permissible bending radius ratio dependence on normalized frequency for the LP_{01} and LP_{11} modes. $\alpha = 4.5$. $\rho = 1$. v_{c2} is the LP_{21} mode cutoff and equals 4.6 for $\alpha = 4.5$. The circle indicates the value at $v = v_{c2}$.

The permissible bending radius of the LP_{11} mode is about three times as large as that of the LP_{01} mode. R^* is also shown for the LP_{01} mode of the step-index fiber with $\alpha = \infty$ and $v = 2.4$. The R^* value of step-index single-mode fiber lies between the R^* values of both modes with $\alpha = 4.5$. The bending radius of the LP_{11} mode at $\Delta = 0.3$ percent is comparable to that of a step-index single-mode fiber with $\Delta = 0.185$ percent. If the core diameters of these fibers are compared, under equal bending radius condition, the dual-mode fiber and the single-mode fiber have 16.3- and 10.7-μm core diameter, respectively.

The normalized frequency dependences of R^* are plotted in Fig. 13 for the LP_{01} and LP_{11} modes with $\alpha=4.5$. The ratio of R^* with two different v values depends only on the ratio of v and is dependent of the combination of λ, Δ, and so on [16]. $v_{c2}=4.605$ is obtained for $\alpha=4.5$. The circle in Fig. 13 implies the value of $v=v_{c2}$. The permissible bending radius of the LP_{11} mode increases more markedly than that of the LP_{01} mode as v decreases.

By making ρ in (1) larger than unity, the core diameter and bending loss will show further improvement. It is expected that the axial offset tolerance will be relaxed with the dual-mode fiber design. Detailed theoretical evaluation of splicing and launching loss is now in preparation.

VI. Conclusion

Detailed design considerations for the broadband dual-mode fiber are presented. Two groups of modes propagate simultaneously and the group delay difference between the LP_{01} and LP_{11} modes vanishes by proper choice of the profile parameters. The normalized frequency v is raised to just below the cutoff of the LP_{21} mode, in order to get as large a core diameter as possible. By choosing the profile parameter $\alpha=4.5$ and the normalized frequency $v=4.6$, a core diameter as large as 16.3 μm is attainable with the relative index difference $\Delta=0.3$ percent at $\lambda=1.25$ μm. Fabrication tolerances to secure group delay difference within 100 ps/km are given by a profile parameter $\alpha=4.85\pm0.25$ and a normalized frequency $v=4.45\pm0.11$.

The material effect of group delay characteristics is investigated to design the practical fibers. The optimum values of α and v depend greatly on the index difference dispersion parameter y rather than on the relative index difference Δ, while the tolerable range depends on Δ rather than y. The tolerable ranges of α and v decrease with Δ. The group delay difference is proportional to the group index N, which, however, is not involved in the determination of optimum condition.

The pulse broadening of the dual-mode fiber is below one seventh that of a highly multimode graded-index fiber, when profile parameter α deviates from optimum value by 5 percent.

The bending loss is studied to show the feasibility of the dual-mode fiber. The bending radius of the LP_{11} mode at $\Delta=0.3$ percent in the dual-mode fiber is comparable to that of a step-index single-mode fiber with $\Delta=0.185$ percent. Under an equal bending radius condition, core diameters of these fibers at $\lambda=1.25$ μm are 16.3 and 10.7 μm, respectively. The dual-mode fiber seems to provide a large-capacity transmission medium with a large core diameter than that of a conventional single-mode fiber.

Appendix I
Calculation of Group Delay [9]

Group delay τ_g for fibers having an α-power refractive-index profile is obtained by the following equations:

$$\tau_g=\frac{N}{c}\cdot\frac{[1-\Delta(1+y/4)\cdot Qx]}{(1-2x\Delta)^{1/2}} \tag{A1}$$

$$N=d(kn)/dk \tag{A2}$$

$$Q=\frac{2v}{u}\cdot\frac{du}{dv}=\frac{4}{\alpha+2}\left[1+\frac{\alpha(1-A)+2(\rho-1)A}{2x(1-A/B)}\right] \tag{A3}$$

$$A=K_m^2(w)/[K_{m-1}(w)K_{m+1}(w)] \tag{A4}$$

$$B=J_m^2(u)/[J_{m-1}(u)J_{m+1}(u)] \tag{A5}$$

$$x=\frac{\alpha+2}{\alpha}\cdot\frac{u^2}{v^2} \tag{A6}$$

$$y=-(2n/N)(\lambda/\Delta)(d\Delta/d\lambda) \tag{A7}$$

where N, c, and y denote the group index, light velocity, and index difference dispersion parameter [10], respectively. J_m and K_m denote the Bessel and modified Bessel functions of order m, respectively. Both u and w are determined by the characteristic equation.

$$\frac{uJ_{m-1}(u)}{J_m(u)}+\frac{\rho-1}{\alpha}u^2=-\frac{wK_{m-1}(w)}{K_m(w)}-\frac{(\rho-1/A)w^2}{\alpha+2} \tag{A8}$$

$$v^2=\frac{\alpha+2}{\alpha}u^2+w^2=2\pi an\sqrt{2\Delta}\ /\lambda. \tag{A9}$$

The index m in (A8) corresponds to the azimuthal mode number of the linearly polarized LP_{ml} mode [8].

Appendix II
Fabrication Tolerances for Core Radius and Relative Index Difference

When both λ and n in (A9) are constants, the relation among fabrication tolerance parameters becomes

$$\frac{\delta v}{v}=\frac{\delta a}{a}+\frac{\delta\Delta}{2\Delta} \tag{B1}$$

where δv, δa, and $\delta\Delta$ are the tolerances of v, a, and Δ, respectively. δv and so on are assumed to be sufficiently small as compared with v and so on. Substitution of relevant parameters into (B1) lead to (5).

Acknowledgment

The authors would like to express their gratitude to K. Noda, G. Marubayashi, Y. Kato, and K. Masuno for their encouragement and to M. Saruwatari for discussions. They are indebted to N. Shibata, S. Shibata, S. Kobayashi, and T. Izawa for offering the refractive-index data on silicate glass.

References

[1] P. Kaiser, G. W. Tasker, W. G. French, J. R. Simpson, and H. M. Presby, "Single-mode fibers with different B_2O_3-SiO_2 compositions," in *Tech. Digest of Topical Meeting on Optical Fiber Transmission II*, 1977, pp. TuD3-1–TuD3-4.

[2] T. Kimura and K. Daikoku, "A proposal on optical fiber transmission systems in a low loss 1.0–1.4-μm wavelength region," *Opt.*

Quantum Electron., vol. 9, no. 1, pp. 33–42, 1977.
[3] S. Kawakami and S. Nishida, "Characteristics of a doubly clad optical fiber with a low-index inner cladding," *IEEE J. Quantum Electron.* vol. QE-10, pp. 879–887, 1974.
[4] J. Sakai, "Transmission characteristics of single-mode fiber with large-core," *Paper of the Tech. Group on Opt. & Quantum Electron.*, IECE of Japan, OQE 76-45, pp. 55–62, 1976.
[5] T. Nakahara, M. Hoshikawa, M. Yoshida, and S. Suzuki, "Transmission properties of ring-type optical fibers," in *Proc. of Second European Conf. Optical Fiber Communication*, 1976, pp. 149–155.
[6] J. Sakai and T. Kimura, "Large-core broadband optical fiber," *Opt. Lett.*, vol. 1, no. 5, pp. 169–171, 1977.
[7] K. Kitayama, M. Ikeda, and Y. Kato, unpublished.
[8] D. Gloge, "Weakly guiding fibers," *Appl. Opt.*, vol. 10, no. 10, pp. 2252–2258, 1971.
[9] K. Okamoto and T. Okoshi, "Analysis of wave propagation in optical fibers having core with α-power refractive index distribution and uniform cladding," *IEEE Trans. Microwave Theory Tech.* vol. MTT-24, pp. 416–421, 1976.
[10] R. Olshansky and D. B. Keck, "Pulse broadening in graded-index optical fibers," *Appl. Opt.*, vol. 15, no. 2, pp. 483–491, 1976.
[11] S. Kobayashi, S. Shibata, N. Shibata, and T. Izawa, "Refractive-index dispersion of doped fused silica," in *Tech. Digest of* Int. Conf. *Integrated Optics and Optical Fiber Communication*, 1977, pp. 309–312.
[12] N. Shibata, S. Shibata, S. Kobayashi, and T. Izawa, private communication.
[13] H. M. Presby and I. P. Kaminow, "Binary silica optical fibers: Refractive index and profile dispersion measurements," *Appl. Opt.*, vol. 15, no. 12, pp. 3029–3036, 1976.
[14] D. Gloge, "Dispersion in weakly guiding fibers," *Appl. Opt.*, vol. 10, no. 11, pp. 2442–2445, 1971.
[15] D. C. Chang and E. F. Kuester, "Radiation and propagation of a surface-wave mode on a curved open waveguide of arbitrary cross section," *Radio Sci.*, vol. 11, no. 5, pp. 449–457, 1976.
[16] J. Sakai and T. Kimura, "Bending loss of propagation modes in arbitrary index profile optical fibers," *Appl. Opt.*, vol. 17, no. 10, pp. 1499–1506, 1978.

A Compact Light-Weight Gaussian-Beam Launcher for Microwave Exposure Studies

PERAMBUR S. NEELAKANTASWAMY, KRISHNA KUMAR GUPTA, AND DILIP KUMAR BANERJEE

Abstract—**A new type of compact light-weight Gaussian-beam launcher for producing a focused-microwave exposure field in biological experiments is described. This launcher is identical to the structure described by the authors elsewhere [1], except that a simple circular waveguide aperture, instead of a corrugated pipe, is used to illuminate a dielectric sphere lens with the result that a considerable weight and size reduction of the launcher is achieved. The proposed structure consists of a simple cylindrical waveguide excited with a balanced mixture of complementary modes and the diffracted field due to this waveguide aperture is made to illuminate a dielectric sphere (lens). It is shown that a near-circular Gaussian beam is then produced in the image space of the sphere with a high focusing factor. Design details, theoretical calculations, and experimental results concerning a practical launcher are presented. Suitability of this compact structure for diathermy applications at a frequency of 2450 MHz is mentioned.**

I. Introduction

RECENTLY, the authors [1], [2] described a practical method of launching a microwave Gaussian beam which is used to produce a focused exposure field in biological experiments for partial-body irradiation. This launcher consists of a dielectric spherical lens, illuminated by a scalar horn; the resulting EM field in the image zone of the lens is a near-circular Gaussian beam. The simplicity and compactness of this structure with its ability to focus microwave energy in a very small region indicate its practical utility in the areas of biological researches and medical applications of microwaves. For example, one of the authors has successfully employed this launcher in a noninvasive beam wave reflectometric instrumentation for measuring complex permittivity of biological materials at microwave frequencies [3].

While the launcher described in [1] is a more practical source of microwave Gaussian beam than the plane-wave irradiated dielectric spherical lens system due to Ho *et al.* [4], yet the sphere-illuminating scalar horn of this launcher is rather a heavy structure, and, therefore, for low-frequency applications (such as for 2450 MHz), there is a need to develop a low-weight launcher system. Hence, presently, a new type of launching device is proposed wherein the heavy scalar horn of [1] is replaced by a suitable low-weight waveguide aperture antenna.

II. Description of the Proposed Structure

Fig. 1 illustrates the launcher structure presently proposed. It consists of an open-ended circular waveguide with a modified aperture end. The open end has a shorted

Manuscript received January 5, 1978; revised March 10, 1978.

P. S. Neelakantaswamy was with the Department of Electrical Engineering, Indian Institute of Technology, Madras 600036, India. He is now with the Electronics Section, School of Applied Sciences, University Science Malaysia, Minden, Penang, Malaysia.

K. K. Gupta and D. K. Banerjee are with the Department of Electrical Engineering, Indian Institute of Technology, Madras 600036, India.

0018-9480/78/0900-0665$00.75 ©1978 IEEE